

Importance of giant spin fluctuations in two-dimensional magnetic trilayers

A. Scherz,* C. Sorg,† M. Bernien, N. Ponpandian, K. Baberschke, and H. Wende
Institut für Experimentalphysik, Freie Universität Berlin, Arnimallee 14, D-14195 Berlin-Dahlem, Germany

P. J. Jensen

Institut für Theoretische Physik, Freie Universität Berlin, Arnimallee 14, D-14195 Berlin-Dahlem, Germany
 (Received 25 January 2005; revised manuscript received 3 May 2005; published 31 August 2005)

Two ultrathin ferromagnetic films of Co and Ni separated by a nonmagnetic spacer of Cu are taken to study the spin-spin correlations of weakly coupled ferromagnets. The Ni film thickness ranging between $d_{\text{Ni}}=2$ and 6 monolayers (ML) is chosen to study the two-dimensional $2\text{D}\rightarrow 3\text{D}$ crossover in ferromagnets. The spacer thickness ranges from $d_{\text{Cu}}=2-8$ ML to monitor the oscillatory behavior of the interlayer exchange coupling. The measured temperature-dependent magnetizations and the corresponding Curie temperatures are accompanied by a microscopic many-body Green's function theory. Both experiment and theory give firm evidence that for nanostructured magnets a static mean field description is insufficient, higher order spin-spin correlations are important and explain the observed increase of the Curie temperature by up to $\sim 200\%$ due to the interlayer exchange coupling. The results are visualized in a three-dimensional diagram as a function of *both* the Ni thickness *and* the Cu spacer thickness.

DOI: 10.1103/PhysRevB.72.054447

PACS number(s): 75.70.Cn, 78.70.Dm, 75.10.Dg

I. INTRODUCTION

Nanostructures of ferromagnetic multilayers and superlattices are a focal point of current research.¹ Obviously, their technological applications are of importance, but they also offer unique features to study fundamental properties in magnetism. For instance, it has been shown that the Curie temperature of an ultrathin Ni film can be shifted by 30% and more when coupled to a second ferromagnetic film.^{2,3} Such a large relative shift in the critical temperature $\Delta T_C/T_C$ has never been observed in bulk magnetism. We investigate prototype “trilayers” to study these effects of two-dimensional (2D) magnets. The trilayers consist of a ferromagnetic layer at the bottom (FM1), a second one on top (FM2), and a nonmagnetic spacer layer (NM) in-between (Fig. 1). These trilayers are the ideal archetype to study the magnetism and the interlayer exchange coupling (IEC) of magnetic multilayers: Via the thicknesses of FM1 and FM2, d_{FM1} and d_{FM2} , respectively, the Curie temperatures can be manipulated. Varying the thickness of NM d_{NM} , changes the strength J_{inter} of the oscillatory IEC.

The IEC is a well-established property of magnetic multilayers.⁴ Its oscillatory character (ferromagnetic, FM, or antiferromagnetic, AFM, coupling between FM1 and FM2) as well as its decreasing strength with increasing spacer thickness d_{NM} have been verified in experiment^{5,6} and theory.⁷ The increasing strength J_{inter} of the IEC with decreasing d_{NM} is represented on the y axis of Fig. 1. In most of the investigations of the IEC in theory and experiment the magnetism of the ferromagnetic film has been treated in a static manner simply considering a mean field approximation. But what will happen with ferromagnetic films with a thickness of a few atomic layers only? Will they order at all? Will higher order spin-spin correlations be important and how will this be influenced by the exchange coupling via the NM spacer? Along the x axis in Fig. 1 we plot the thickness of the ferromagnetic bottom layer FM1. It is clear that with

decreasing thickness also the Curie temperature T_C decreases, following the *finite size scaling*.⁸ When a three-dimensional (3D) bulk solid is reduced to 2D, the correlation length close to the phase transition may get larger than the geometrical dimensions. The spin-spin correlation can be taken only over a 2D plane missing the correlations in the third dimension. All this leads to an increase of fluctuations and a reduction of the critical temperature T_C – in the extreme limit to $T_C\rightarrow 0$. But how will this be influenced if the ferromagnetic layer FM1 is exchange coupled to a second ferromagnetic film FM2? Is it only the static exchange field of FM2 which acts on the magnetization of FM1 (field induced magnetization)? It has been shown that this static mean field picture is insufficient to describe magnetic correlations of ultrathin ferromagnets.⁹⁻¹² Static exchange fields of realistic values will shift T_C only by a few kelvin. The observed shift ΔT_C is much larger. We plot ΔT_C along the z axis of the schematic diagram in Fig. 1 as a measure of higher order spin-spin correlations.

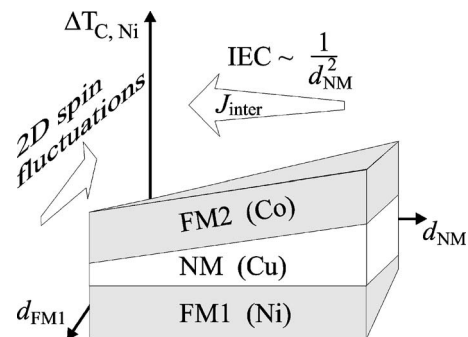


FIG. 1. Schematic illustration of a ferromagnetic two wedge trilayer. $\Delta T_{C,\text{Ni}}$ is controlled by two independent parameters: (i) the IEC depending on d_{NM} , and (ii) the thickness d_{FM1} , while d_{FM2} is kept constant.

It is the purpose of the present work to combine both effects which are schematically indicated in the three-dimensional plot in Fig. 1. We investigate the temperature dependence of the element-specific magnetization curves for different sets of samples, in each case varying the thickness of one constituent and keeping the others constant. Scanning along the d_{FMI} axis (using wedge or staircase films) and keeping d_{NM} constant modifies the strength of the 2D correlations. Keeping d_{FMI} constant and varying d_{NM} monitors the oscillatory character of the IEC. The two strongly interrelated, competing effects may dramatically influence the critical behavior in the limits indicated by the arrows in Fig. 1, i.e., $d_{\text{FMI}} \rightarrow 0$ and $d_{\text{NM}} \rightarrow 0$. To clarify the notation we label the Curie temperature of a single Ni film $T_{\text{C,Ni}}$ and the shifted value $T_{\text{C,Ni}}^*$, to indicate that in a strict thermodynamic sense the latter may not refer to a real phase transition. Nevertheless, in a practical situation it makes sense to call $T_{\text{C,Ni}}^*$ a quasicritical temperature.^{2,3} Bergqvist and Eriksson¹³ have calculated the spin-spin correlations for such a weakly coupled 2D ferromagnet. They conclude that the spin-spin correlations above $T_{\text{C,Ni}}^*$ are very small and the Ni magnetization (order parameter) vanishes.¹³

Before describing the experimental and theoretical methods in detail we review previous results on Co/Cu/Ni/Cu(100) trilayers and related systems. The growth and magnetic properties of this system, as well as the ones of the individual Ni and Co ultrathin films on Cu(100), have been measured in detail.^{14–17} X-ray magnetic circular dichroism (XMCD) allows for the determination of the element-specific magnetization of each film individually. Two peaks in the ac susceptibility have been measured.² The onset of magnetic order in the Ni and Co films was determined by photoemission electron microscopy.¹⁸ These experiments reveal that the interlayer coupling induces a strong magnetization into the material with the lower T_{C} .^{2,9,10,18–22} Even for very weak applied fields ($H \sim 8$ kA/m) pronounced magnetization changes have been observed for a Co/Cu(100) ultrathin film system,¹¹ which is impossible to provoke in bulk-like magnets. Depending on the Ni and Co film thicknesses three different situations may occur: (i) $T_{\text{C,Ni}} < T_{\text{C,Co}}$,^{2,22,23} (ii) $T_{\text{C,Ni}} > T_{\text{C,Co}}$,²⁰ and (iii) $T_{\text{C,Ni}} \sim T_{\text{C,Co}}$.²¹ Recently, at room temperature the corresponding boundaries between the different cases have been established for cross-wedged Co/Cu/Ni/Cu(100) trilayers.¹⁸

The paper is organized as follows. In Secs. II and III experiments and calculations are described. In Sec. IV measured and calculated results for the Ni magnetization curve of the Cu/Ni bilayer and the Co/Cu/Ni trilayer are presented. As a main result we combine the two effects (IEC and 2D ferromagnet) in a 3D diagram yielding a quantitative description of $\Delta T_{\text{C,Ni}}/T_{\text{C,Ni}}$ as a function of the *two* variables d_{Ni} and d_{Cu} . Note that this combination is only possible after treating $M(T)$ close to $T_{\text{C,Ni}}^*$ in an appropriate manner by considering the nonlinearity between $\Delta T_{\text{C,Ni}}/T_{\text{C,Ni}}$ and J_{inter} .

II. EXPERIMENTAL DETAILS

The *in situ* preparation and measurements of the Co/Cu/Ni/Cu(100) system are performed in ultrahigh

vacuum conditions (base pressure $p < 2 \times 10^{-10}$ mbar). The single-crystal Cu(100) substrate was cleaned in a conventional way by Ar⁺ sputtering and annealing to 900 K. The trilayers were prepared at room temperature by evaporating the material from high purity metal rods. Ni/Cu(100) films show a pseudomorphic layer-by-layer growth up to 5 ML with marginal interdiffusion.^{14,15} The Cu spacer thickness d_{Cu} ranges from 2–8 ML in order to limit the interface roughness. On top of the spacer layer a Co film is deposited, which also exhibits a layer-by-layer growth mode. The thicknesses d_{Co} and d_{Ni} of the Co and Ni films are chosen such that their Curie temperatures $T_{\text{C,Co}}$ and $T_{\text{C,Ni}}$ are located in a convenient temperature range of about 30–330 K. The upper temperature limit is related to the onset of interdiffusion processes at the interfaces. When capped by Cu the Curie temperature of a Ni film drops by several 10 K due to hybridization effects at the Cu/Ni interface.^{24,25} Thus, the Cu/Ni/Cu(100) bilayers with two to six Ni atomic layers have $T_{\text{C,Ni}} \approx 30\text{--}275$ K. The Curie temperature $T_{\text{C,Co}}$ of the Co films with one to three layers ranges from 50–580 K.

The absorption spectra are measured via the total electron yield of the sample. The individual magnetizations are probed by tuning the photon energy to the Ni and Co $L_{2,3}$ absorption edges, respectively. The experiments were carried out at the UE56/2-PGM1 beamline of the Berlin synchrotron radiation facility BESSY II. The high brilliance of circularly polarized x-rays of this source provides a sufficient sensitivity to resolve very small magnetic signals. This enabled us, unlike in previous studies,^{2,3} to observe the IEC-induced magnetization tails of Ni which provides further insight into the magnetic behavior of the exchange coupled trilayers as discussed below.

The absolute values for the magnetization of the samples were determined by comparing the XMCD spectra of the films with the one of a bulk reference sample measured under the same experimental conditions. The temperature dependence of the individual magnetizations was deduced once with the absorption spectra at each temperature point. For all other samples the magnetization curves were then collected correspondingly by probing the asymmetry of the absorption at the L_3 edge with respect to the L_3 preedge absorption for both magnetization directions at fixed helicity of the incident light. All investigations in the present study are performed by applying a weak magnetic field of $H \approx 3$ kA/m, to rule out the existence of magnetic domains that may persist in ultrathin Ni films in a wide temperature range.²⁶ This magnetic field is sufficiently large to saturate the sample magnetization close to $T_{\text{C,Ni}}$, and is small enough not to induce a sizable tail in the magnetization curve.^{22,23} Hence, the measured temperature shift of the Ni magnetization is caused almost exclusively by the IEC.

III. THEORETICAL MODEL

For the interpretation of the experiments we apply a Heisenberg Hamiltonian considering the isotropic exchange, the Zeeman term, and the dipole interaction,

$$\mathcal{H} = -\frac{1}{2} \sum_{\langle i,j \rangle} J_{ij} \mathbf{S}_i \mathbf{S}_j - \mu_0 \mathbf{H} \sum_i \boldsymbol{\mu}_i + \frac{\mu_0}{2} \sum_{\substack{i,j \\ i \neq j}} \frac{1}{r_{ij}^5} [\boldsymbol{\mu}_i \boldsymbol{\mu}_j r_{ij}^2 - 3(\mathbf{r}_{ij} \boldsymbol{\mu}_i)(\mathbf{r}_{ij} \boldsymbol{\mu}_j)]. \quad (1)$$

A fcc(100) thin film system with thickness $d = d_{\text{Ni}} + d_{\text{Co}}$ is assumed. Note that we can consider only films with full layers (integer thickness). \mathbf{S}_i denotes a localized quantum spin with spin number $S=1$ on lattice site i and with layer-dependent magnetic moments $\boldsymbol{\mu}_i = \mu_i \mathbf{S}_i / S$ taken from experiments.^{16,17} An in-plane magnetization $\langle \mathbf{S}_i \rangle = \mathbf{M}_i(T)$ parallel to the external magnetic field \mathbf{H} is assumed. The distance between sites i and j is given by $|\mathbf{r}_{ij}| = r_{ij}$, and μ_0 is the vacuum permeability. The wave-vector dependent lattice sums are determined by the Ewald summation technique.²⁷ Furthermore, due to competing lattice anisotropies and dipole interaction the single Ni/Cu(001) thin film system exhibits an interesting spin reorientation behavior with increasing thickness and temperature.⁸ Whereas the surface anisotropy and the dipole coupling prefer an in-plane magnetization, the strain-induced lattice anisotropy of the interior film layers prefers a perpendicular one. The considered thicknesses in the present study always refer to an in-plane magnetic orientation. However, we note that as long as an in-plane magnetization is guaranteed, an explicit consideration of the lattice anisotropy as discussed in detail in Ref. 28 will not vary the results significantly. The reason is that for a 2D ferromagnet the Curie temperature depends only logarithmically on the actual values of the anisotropies.²⁹ Thus, for simplicity an additional lattice anisotropy is not taken into account in the present study.

The isotropic exchange interaction J_{ij} couples nearest-neighbor spins in the same layer and between neighboring layers, as sketched in Fig. 2. In order to account for the hybridization effects in particular at the Ni/Cu interfaces where the magnetic moment of Ni is markedly reduced,^{16,30} we assume different exchange couplings for the interface and the interior film layers, $J_{\text{Ni}}^{\text{interior}} = 15.3$ meV/bond and $J_{\text{Ni}}^{\text{interface}} = 3.1$ meV/bond. The direct coupling of the inner layers is the Ni bulk value, whereas the value at the interface is determined such that the model reproduces the measured $T_{\text{C,Ni}}(d_{\text{Ni}})$ (see below, Fig. 5). For the Co layer an averaged value $J_{\text{Co}} = 34.3$ meV/bond is used for all Co spin pairs since (i) in Co the effect is less pronounced as in Ni, (ii) the reduction of the Co moment at the Co/Cu interface is approximately canceled out by the enhancement of the moment in the topmost layer facing vacuum,¹⁷ and finally, (iii) assuming layer-resolved values for Co will hardly change the results obtained for the Ni magnetization. These intralayer couplings are used for all calculations, if not stated otherwise. Magnetic moments are taken from experiments,^{16,17} layer dependent in the case of Ni, an average in the case of Co. The Ni and Co layers are coupled by the IEC J_{inter} across the Cu spacer layer, where for simplicity a single Ni spin at the Ni/Cu interface is coupled to a single Co spin at the Co/Cu interface. A dispersion of the IEC is not considered.

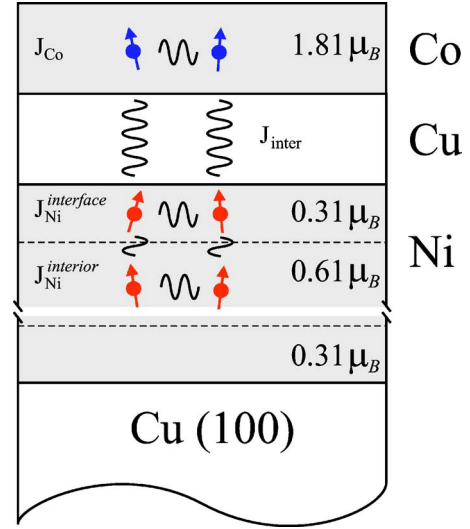


FIG. 2. (Color online) Sketch of the investigated Co/Cu/Ni/Cu(100) trilayers and the underlying assumptions for the theoretical model. Magnetic moments are taken from experiments (Refs. 16 and 17).

Since for layered magnets it is important to take collective magnetic excitations (spin waves) into account, we apply a many-body Green's function approach for the calculation of the layer-dependent magnetizations.^{29,31} The following Green's functions in energy space are used

$$G_{ij}^{+-(n)}(\omega, \mathbf{k} ||) = \langle \langle S_i^+; (S_j^-)^n S_j^- \rangle \rangle_{\omega, \mathbf{k}}, \quad (2)$$

where the operator $(S_j^-)^n S_j^- = C_j^{(n)}$ is introduced to consider arbitrary spin quantum numbers ($0 \leq n \leq 2S-1$).³¹ A Fourier transformation into the 2D momentum space with wave vector $\mathbf{k} ||$ has been performed, the labels i and j in Eq. (2) refer to the layer index.

Higher-order Green's functions appearing in the equations of motion are approximated by the Tyablikov decoupling³² (random phase approximation, RPA) of the exchange and dipole interaction terms ($i \neq k$)

$$\langle \langle S_i^+ S_k^+; C_j^{(n)} \rangle \rangle \approx \langle S_i^+ \rangle \langle \langle S_k^+; C_j^{(n)} \rangle \rangle = M_i(T) G_{kj}^{+-(n)}. \quad (3)$$

This approximation allows to calculate the magnetization not only at low temperatures, as in the free spin wave theory,³³ but can also be applied at elevated temperatures, since interactions between magnons are partly taken into account. Satisfactory results are obtained for the ordering temperatures. The expectation values $M_i(T)$ are determined from the spectral theorem.²⁹

IV. RESULTS AND DISCUSSION

Let us first summarize our experimental results. To investigate separately the dependence of the different film thicknesses on the shift of the critical temperature of Ni, we have prepared staircase trilayers in which the thickness of one constituent is varied in macroscopic steps of ~ 2 nm width and the others are kept constant. With the example shown in Fig. 3 we demonstrate how the influence of the IEC on the

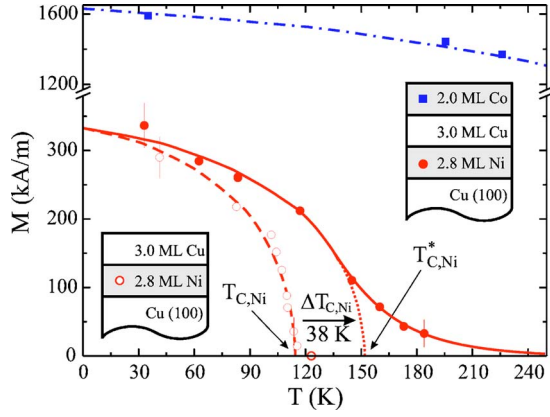


FIG. 3. (Color online) Ni (circles) and Co (squares) sublayer magnetizations $M_{\text{Ni}}(T)$ and $M_{\text{Co}}(T)$ probed by XMCD. The influence of the IEC J_{inter} on the Ni magnetization is monitored by comparing $M_{\text{Ni}}(T)$ before (open symbols) and after (closed symbols) the deposition of the Co film. The solid and dot-dashed lines are guides to the eye. A standard Ni magnetization curve (see text) is fitted to the Ni data points (dashed and dotted lines), yielding $T_{\text{C,Ni}}$ and $T_{\text{C,Ni}}^*$.

magnetization and the critical behavior in the vicinity of $T_{\text{C,Ni}}$ is characterized: First the Ni magnetization curve (open circles) is measured for the capped Cu/Ni/Cu(100) film. Then 2 ML of Co are deposited having $T_{\text{C,Co}} \approx 320$ K larger than $T_{\text{C,Ni}}$. The shift $\Delta T_{\text{C,Ni}} = T_{\text{C,Ni}}^* - T_{\text{C,Ni}}$ is obtained after investigating the Ni magnetization of the trilayer. Note that the shift is always directed toward higher temperatures, regardless whether the Ni and Co magnetizations are aligned

parallel or antiparallel.^{34,35} In the present study, the shift is derived with the help of a standard magnetization curve³ (dashed line), which has been obtained from various measurements of thin Ni/Cu(100) films in the thickness range 3–5 ML. A fit of this standard curve to the data points allows for a determination of $T_{\text{C,Ni}}$ with an accuracy of a few kelvin. In order to define the temperature shift caused by the IEC, we use the same standard curve (dotted line) for a fit to the data points of the Ni magnetization in the coupled trilayer system, yielding the “quasicritical temperature” $T_{\text{C,Ni}}^*$. This temperature refers to the resonancelike maximum of the susceptibility.² Using this procedure, we find $\Delta T_{\text{C,Ni}} \approx 38$ K for the example given in Fig. 3. The corresponding results of $\Delta T_{\text{C,Ni}}$ for all investigated samples are summarized in Table I. They are sorted in three groups: (i) the dependence on the Ni film thickness d_{Ni} , (ii) the dependence on the Cu spacer thickness d_{Cu} , and (iii) some dependence on the Co film thickness d_{Co} and thus on $T_{\text{C,Co}}$.

Using the Green’s function theory (GFT) we have calculated $M(T)$ for a number of different trilayer systems. As an example we present in Fig. 4 the case corresponding to the experiment of Fig. 3. Comparable lines are plotted with the same style in both figures. We determine $T_{\text{C,Ni}} = 151$ K, which is somewhat larger than the measured one in Fig. 3. Introducing an IEC to the Co film yields a shift of the critical temperature of Ni to higher temperatures. Using $J_{\text{inter}} = 86 \mu\text{eV}/\text{bond} \approx 1 \text{ K}/\text{bond}$ and applying $M_{\text{Ni}}(J_{\text{inter}}=0)$, as described in Sec. II, we obtain $T_{\text{C,Ni}}^* = 188$ K and the shift $\Delta T_{\text{C,Ni}} = 37$ K, in accordance with the measured one. The determined value of the IEC is of the same order of magnitude as obtained from recently measured Ni/Cu/Co/Cu(100) trilayers by ferromagnetic resonance (FMR).⁵

TABLE I. Measured ordering temperatures of the Ni films in Cu/Ni/Cu(100) and Co/Cu/Ni/Cu(100), and the resulting $\Delta T_{\text{C,Ni}} = T_{\text{C,Ni}}^* - T_{\text{C,Ni}}$. The systems marked by a † refer to samples with a staircase layer of either Ni or Co. The accuracy of the thickness calibration, given in monolayer (ML) equivalents, is estimated to be 5%. The fourth column denotes whether the Ni and Co films are coupled ferromagnetic (FM) or antiferromagnetic (AFM) to each other. Note that some samples are listed twice for a better comparison of the results.

Bi- and trilayers				$T_{\text{C,Ni}}$ (K)	$T_{\text{C,Ni}}^*$ (K)	$\Delta T_{\text{C,Ni}}$ (K)	$\Delta T_{\text{C,Ni}}/T_{\text{C,Ni}}$
Ni (ML)	Cu (ML)	Co (ML)	IEC				
Ni dependence							
†2.1	4.2	3.0	AFM	30(15)	100(5)	70(16)	2.3(17)
†3.1	4.2	3.0	AFM	147(16)	214(5)	67(17)	0.46(16)
†4.2	4.2	3.0	AFM	237(13)	314(5)	77(14)	0.32(7)
2.6	3.3	2.4	AFM	85(18)	175(5)	90(19)	1.1(5)
2.8	3.0	2.0	FM	114(6)	152(5)	38(8)	0.33(8)
3.8	3.0	2.0	FM	223(2)	251(6)	28(6)	0.13(3)
Cu dependence							
2.8	3.0	2.0	FM	114(6)	152(5)	38(8)	0.33(8)
2.8	6.2	2.0	AFM	117(2)	141(5)	24(5)	0.21(5)
2.8	7.0	2.0	AFM	114(6)	132(5)	18(8)	0.16(8)
2.8	7.8	2.0	FM	111(3)	138(4)	27(5)	0.24(5)
Co dependence							
†3.1	4.2	2.2	AFM	147(16)	170(5)	23(17)	0.16(13)
†3.1	4.2	1.5	AFM	147(16)	156(5)	9(17)	0.06(12)

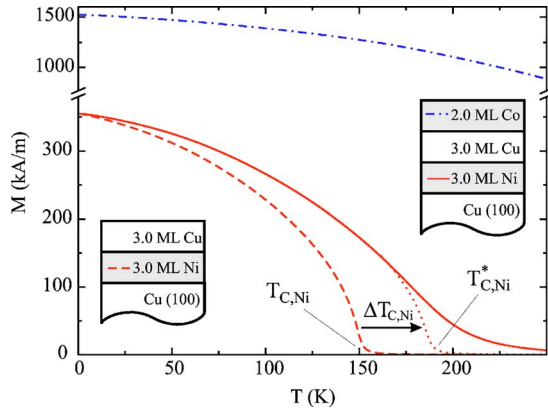


FIG. 4. (Color online) Calculated Ni magnetization of a single Ni film (dashed line) and of a Ni film coupled to a Co film (solid line) as a function of the temperature with $J_{\text{inter}}=86 \mu\text{eV}/\text{bond}$, corresponding to the experiment shown in Fig. 3. The dot-dashed line refers to the Co magnetization. An external magnetic field of $H=3 \text{ kA/m}$ causes the small tail in the Ni magnetization of the bilayer. By applying $M_{\text{Ni}}(J_{\text{inter}}=0)$, see text, we identify $T_{\text{C,Ni}}^*$ (dotted line) and $\Delta T_{\text{C,Ni}}=37 \text{ K}$.

The interplay between the IEC and the dimensionality (thickness of FM1) will now be studied in detail. Therefore, we first have a look at $T_{\text{C,Ni}}$ and $T_{\text{C,Ni}}^*$ as shown in Fig. 5. We plot $T_{\text{C,Ni}}^*$ given in the first three rows of Table I as full circles. These values of Co/Cu/Ni/Cu(100) are determined in one experiment with a staircase Ni film of three thicknesses. The chosen Co film thickness $d_{\text{Co}}=3 \text{ ML}$ ensures $T_{\text{C,Co}} \gg T_{\text{C,Ni}}$. The strength of the IEC is kept constant, i.e., $d_{\text{Cu}}=\text{const}$. To visualize the effect of the IEC we plot $T_{\text{C,Ni}}$ of separate experiments of Cu/Ni/Cu(100) as open circles. It is clearly seen that the datapoints for the full trilayer are systematically larger than the ones of the capped single film. Certainly, in real experiments we are not able to reduce the

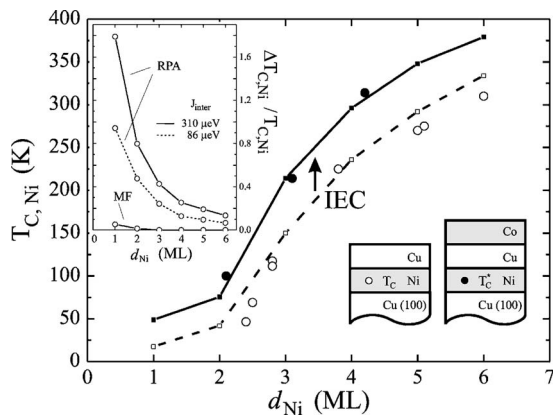


FIG. 5. $T_{\text{C,Ni}}$ and $T_{\text{C,Ni}}^*$ as functions of the Ni film thickness d_{Ni} of bilayers and trilayers (experiment: open and full circles, theory: solid and dashed lines). The IEC is determined to be $J_{\text{inter}}=310 \mu\text{eV}/\text{bond}$. In the inset the relative temperature shift $\Delta T_{\text{C,Ni}}/T_{\text{C,Ni}}(d_{\text{Ni}})$ is shown highlighting the difference between the calculations with (RPA) and without (MF) consideration of collective magnetic excitations.

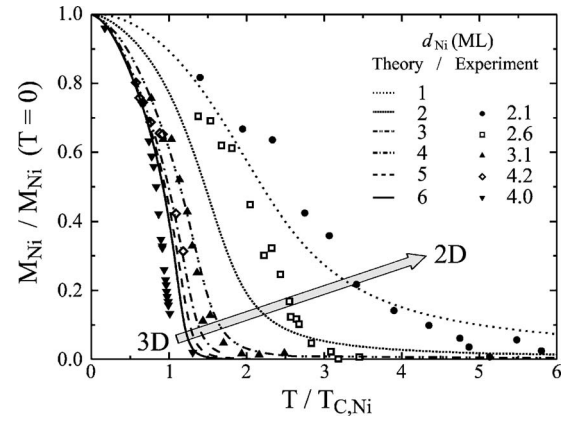


FIG. 6. Magnetization $M_{\text{Ni}}(T)/M_{\text{Ni}}(T=0)$ as a function of the relative temperature $T/T_{\text{C,Ni}}(d_{\text{Ni}})$ scaled by the corresponding Curie temperature of the capped Ni films. For the calculations $J_{\text{inter}}=310 \mu\text{eV}/\text{bond}$ and $d_{\text{Co}}=3 \text{ ML}$ are used. The cases with Ni thicknesses of 2.1, 2.6, 3.1, and 4.2 ML and the corresponding Co and Cu thicknesses are given in Table I. The top-down triangles ($d_{\text{Ni}}=4.0 \text{ ML}$) represent a case without IEC ($J_{\text{inter}}=0$).

thickness below 2 ML. The corresponding GFT calculations were carried out from 1 to 6 ML of Ni. The Curie temperatures of the capped single films (dashed line) as well as $T_{\text{C,Ni}}^*$ of the trilayer (solid line) agree almost perfectly with the experimental finding. The inset of Fig. 5 shows the relative shift $\Delta T_{\text{C,Ni}}/T_{\text{C,Ni}}(d_{\text{Ni}})$ calculated with (RPA) and without (MF) consideration of collective magnetic excitations, i.e., higher order spin-spin correlations. Two important features in Fig. 5 are noted: (i) We see that a single Ni film remains FM with finite $T_{\text{C,Ni}}$ even down to $d_{\text{Ni}}=1 \text{ ML}$ (experimentally not accessible). (ii) We find that $\Delta T_{\text{C,Ni}}$ ranges between ~ 30 and 70 K . Certainly, an increase by $\sim 30\text{--}70 \text{ K}$ of a critical temperature of $\sim 20 \text{ K}$ only, is more dramatic than the same shift of a critical temperature of $\sim 300 \text{ K}$. In other words, although the absolute shift looks approximately constant the important finding is that higher order spin-spin correlations shift the magnetic ordering temperature of the ultrathin 2D-like film relatively by up to about 200% for 2 ML (see last column of Table I)—never accessible in 3D bulk.

The increasing influence of the IEC on $M_{\text{Ni}}(T)$ with decreasing d_{Ni} is also illustrated in Fig. 6. We plot M_{Ni} normalized to $M_{\text{Ni}}(T=0)$ as a function of T normalized to $T_{\text{C,Ni}}(J_{\text{inter}}=0)$. Again the GFT calculations (lines) show that the increase of M_{Ni} close to the Curie temperature gets more dramatic the thinner the Ni film. Obviously, this tail is particularly pronounced for 1 ML Ni (dotted line). This cannot be explained simply by the static exchange field³⁶ of the top Co film but only by taking higher order spin-spin correlations into account. The four experimental cases with a Ni thickness of 2.1, 2.6, 3.1, and 4.2 ML are the ones given in the first four rows of Table I. The curve given by the top-down triangles ($d_{\text{Ni}}=4.0 \text{ ML}$) represents a case without IEC ($J_{\text{inter}}=0$). Thus, the change of the magnetization of the trilayers can be seen by comparing their $M_{\text{Ni}}(T)$ to the one

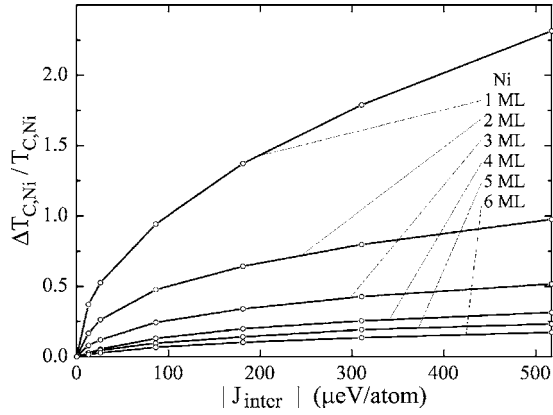


FIG. 7. Relative temperature shift $\Delta T_{C,Ni}/T_{C,Ni}$ of the Ni magnetization as a function of the strength of the IEC $|J_{inter}|$.

with the top-down triangles. Measuring M_{Ni} close to $T_{C,Ni}^*$ is rather difficult and a scatter of the data points is no surprise. However, the same trend as in theory is evident: The thinnest film of $d_{Ni}=2.1$ ML (full circles) shows a much larger tail than the thickest film of $d_{Ni}=4.2$ ML (open diamonds). Although the experimental and theoretical results differ in the 3D to 2D crossover by approximately 1 ML, the overall agreement is clearly visible.

As a focal point of the present paper, we determine the full dependence of the shift $\Delta T_{C,Ni}/T_{C,Ni}=f(d_{Ni},d_{Cu})$. As sketched in Fig. 1, for a comprehensive interpretation of $\Delta T_{C,Ni}$ in magnetic trilayers with ultrathin Ni films one has to take into account both the magnetic fluctuations for $T>0$ and the spacer-thickness-dependent IEC. The influence of d_{Cu} on $\Delta T_{C,Ni}$ has been explored in previous experimental studies.³⁴ Here we assume that the variation of d_{Cu} solely affects J_{inter} , and not the intralayer couplings J_{Co} and J_{Ni} . At $T=0$ the oscillatory dependence of the IEC on d_{Cu} is given by Bruno's expression^{7,37}

$$J_{inter}(d_{Cu}) = \sum_n \frac{A_n}{d_{Cu}^2} \sin(k_n d_{Cu} + \phi_n). \quad (4)$$

The calculated short- and long-period oscillations $\Lambda_n = 2\pi/k_n$ and the phase shifts ϕ_n have been well reproduced by experiments,^{34,38} yielding $\Lambda_1=2.56$ ML with $\phi_1=\pi/2$ and $\Lambda_2=5.88$ ML with $\phi_2=\pi$ for a Cu(100) spacer, respectively. The ratio of the amplitudes is obtained from measurements to be $A_1/A_2=1.3(5)$. Thus, the only free parameter is the absolute value A_1 in Eq. (4), which will be determined with the help of our theory by comparison to experimental results. Moreover, the influence of the Co film thickness will be addressed, since obviously the effective strength of the IEC depends also on the magnetic order of the Co film and thus on its Curie temperature. For this purpose we calculate first the relative temperature shift $\Delta T_{C,Ni}/T_{C,Ni}$ as a function of $|J_{inter}|$ for different thicknesses of the Ni film. As can be observed from Fig. 7, a nonlinear behavior results, in particular for small d_{Ni} . These results indicate again that magnetic fluctuations are efficiently suppressed even by small coupling strengths ~ 100 $\mu\text{eV}/\text{bond}$.

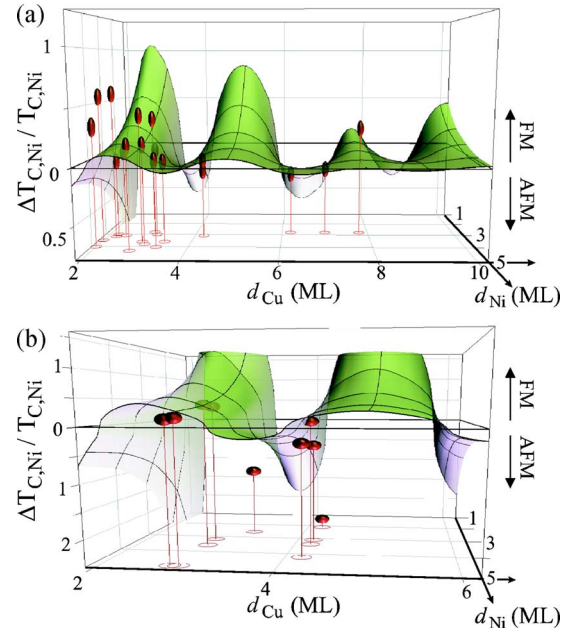


FIG. 8. (Color online) Two-parameter plot of the relative temperature shift $\Delta T_{C,Ni}/T_{C,Ni}(d_{Ni},d_{Cu})$ for Co/Cu/Ni/Cu(100) trilayers as a function of the Ni film thickness d_{Ni} and the thickness d_{Cu} of the Cu spacer layer. Two different thicknesses of the Co film are assumed: (a) $d_{Co}=2$ ML and (b) $d_{Co}=3$ ML.

Now we are in a position to combine our theoretical and experimental findings: The suppression/enlargement of the spin fluctuations, visualized in the relative shift $\Delta T_{C,Ni}/T_{C,Ni}$, depends on the one hand on d_{Ni} (2D character of FM1). On the other hand it depends on the strength of the IEC, i.e., $|J_{inter}|$. Combining both variables we end up in a 3D plot as anticipated at the beginning. The result is a curved surface of $\Delta T_{C,Ni}/T_{C,Ni}=f(d_{Ni},d_{Cu})$. The experimental data of Table I together with results of earlier investigations are shown as full dots and in the projection to the $d_{Ni}-d_{Cu}$ plane (open circles). They are sorted into two groups: $d_{Co}=2$ ML in Fig. 8(a) and $d_{Co}=3$ ML in Fig. 8(b). The zero plane is given by $J_{inter}=0$. Note that the difference of $\Delta T_{C,Ni}/T_{C,Ni}$ with respect to the zero plane refers always to a *positive* temperature shift. We have chosen this kind of illustration to distinguish regions with a parallel arrangement of the two FM layers ($J_{inter}>0$, above the zero-plane) from the ones with an anti-parallel alignment ($J_{inter}<0$, below the zero plane). The envelope of $\Delta T_{C,Ni}/T_{C,Ni}$ as a function of the Cu spacer thickness decreases approximately as d_{Cu}^{-2} for Ni thicknesses $d_{Ni} \geq 5$ ML. For thinner Ni films $\Delta T_{C,Ni}/T_{C,Ni}$ decreases more softly due to the nonlinear scaling with J_{inter} (Fig. 7). The agreement between experimental and theoretical results for $\Delta T_{C,Ni}/T_{C,Ni}$ is reasonably well for $d_{Ni} \geq 3$ ML and $d_{Cu} \geq 3$ ML (Fig. 8). (Differences at ~ 2 ML of Ni and Cu, respectively, between the experimental results and the theory may be due to metallurgical problems.)

Matching the calculated relative temperature shifts $\Delta T_{C,Ni}/T_{C,Ni}$ to the experimental data the IEC can be quantitatively derived. The amplitude of the short-period oscillation is obtained to be $A_1(d_{Co}=2 \text{ ML})=1.0$ meV/bond by fitting the experimental results given Fig. 8(a). This value

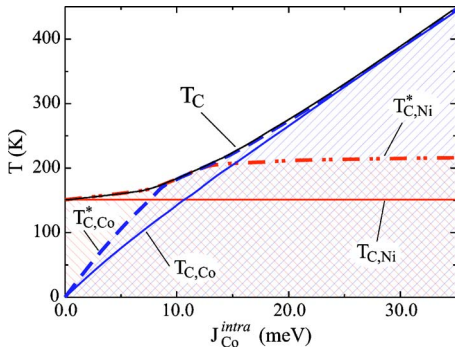


FIG. 9. (Color online) Calculated phase diagram of the Co/Cu/Ni trilayer system. The Curie temperatures T_C , $T_{C,Ni}$, and $T_{C,Co}$, and the quasicritical temperatures $T_{C,Ni}^*$ and $T_{C,Co}^*$ are shown as a function of the exchange coupling J_{Co} in the Co film.

corresponds to a coupling energy of $J_{inter}(T=0, d_{Cu}=5 \text{ ML}) = 63 \mu\text{eV}/\text{bond}$. Comparing this value to results from FMR measurements with $d_{Co}=2 \text{ ML}$ (Ref. 39) we find fair agreement. Since the FMR data were recorded at room temperature they have to be extrapolated to $T=0$. Interestingly, determining A_1 for $d_{Co}=3 \text{ ML}$ [by fitting to the experimental data of Fig. 8(b) by the same procedure] yields a 10 times larger value as compared to the previous case. Such a large variation of $A_1(d_{Co})$ is not expected by just increasing the thickness of the Co film. This effect may be related to some deficiencies of our study which depend on approximations of the theoretical model. In our model we separate only the direct intralayer coupling of Ni into a bulk and an interface component ($J_{Ni}^{interior}$ and $J_{Ni}^{interface}$). However, a more advanced model might include a complete thickness dependence of J_{Co} and J_{Ni} . Such a variation due to quantum well states has been determined.^{25,40} Also the use of a Heisenberg Hamiltonian with localized spins represents an approximation to the present itinerant-electron magnets Ni and Co, although such a model reproduces a number of important features (e.g., Bloch- $T^{3/2}$ law for the decrease of the bulk magnetization, Curie-Weiss behavior of the susceptibility for $T > T_C$, etc.) Moreover, the applied Tyablikov decoupling could underestimate the effect of spin fluctuations in particular for 2D systems, which should be tested by improved approximations beyond RPA.⁴¹ We note that the present theoretical calculation and the one in Ref. 28 give quantitatively satisfactory results if the anisotropies are much smaller than the exchange coupling. For ultrathin films out-of-plane magnetocrystalline anisotropies may be important. Recently, Schwieger *et al.* have published an advanced theory²⁸ in which exchange and magnetic anisotropy couplings are treated on equal footing. Future treatments within this theory will be advisable to further analyze the experimental results of this work. Furthermore, finite experimental inhomogeneities, such as roughness and noninteger film thicknesses in the trilayer, could sensitively change the $T_{C,Ni}$ and J_{inter} with d_{Cu} as well as with d_{Ni} . This is of particular importance when approaching the ultrathin film limit for both Ni and Cu, where the strongest effects are expected on the Ni magnetization.

In Fig. 9 we show the calculated phase diagram of the

Co/Cu/Ni trilayer system in the $T-J_{Co}$ plane. The various characteristic temperatures of trilayer systems T_C , $T_{C,Ni}$, $T_{C,Ni}^*$, $T_{C,Co}$, and $T_{C,Co}^*$ are plotted as functions of the direct exchange coupling J_{Co}^{intra} in the top Co film. The parameters of the calculation are $d_{Ni}=3 \text{ ML}$, $d_{Co}=2 \text{ ML}$, and $J_{inter}=310 \mu\text{eV}/\text{bond}$. The dependence on J_{Co}^{intra} can be discussed between the following limits: $J_{Co}^{intra}=0$ corresponds to a system without Co, yielding the Curie temperature $T_{C,Ni}=150 \text{ K}$ of a single Ni film capped with Cu. The right-hand side of $J_{Co}^{intra} \approx 34 \text{ meV}$ corresponds to a realistic exchange coupling of 2 ML Co.²² Four areas that are separated by the curves of the quasicritical temperatures $T_{C,Ni}^*$ (dash-dotted line) and $T_{C,Co}^*$ (dashed line) can be identified in Fig. 9: In the white area both films are paramagnetic and the whole trilayer is above its transition temperature T_C . In the light shaded fields one film is FM and the other one is paramagnetic. Both films are ordered ferromagnetically in the dark shaded area. In the shaded areas three relevant cases can be distinguished: (i) For $J_{Co}^{intra} \lesssim 9 \text{ meV}$ the quasicritical temperature of Co $T_{C,Co}^* < T_{C,Ni}$. $T_{C,Co}$ is shifted up to $T_{C,Co}^*$ by the IEC. Interestingly, even a small increase of $T_{C,Ni}$ is visible. (ii) In the range of $9 \text{ meV} \lesssim J_{Co}^{intra} \lesssim 13 \text{ meV}$ the two quasicritical temperatures $T_{C,Co}^*$ and $T_{C,Ni}^*$ coincide. The Curie temperatures of both Ni and Co are sizeably enhanced. (iii) The strongest increase of $T_{C,Ni}$ is found in the region $J_{Co}^{intra} \geq 13 \text{ meV}$ where $T_{C,Co} > T_{C,Ni}^*$. In this regime we carried out the investigations of the present work.

V. SUMMARY

At first glance, one might assume that in an archetype trilayer as depicted in Fig. 1 the top Co film simply serves as a magnetic field applied to the lower Ni film. Here we show that this simple picture does not hold in the 2D limit. We present a systematic experimental and theoretical study for the IEC-induced shift $\Delta T_{C,Ni}$ as a function of *both* d_{Ni} and d_{Cu} in coupled magnetic Co/Cu/Ni/Cu(100) trilayers. In particular for very thin Ni films quite large relative shifts $\Delta T_{C,Ni}/T_{C,Ni}$ of more than 200% are observed. This can only be explained by the *action of enhanced spin fluctuations* in these two-dimensional magnets. The IEC between the two ferromagnetic films suppresses efficiently these spin fluctuations and induces a sizable magnetization in the Ni film. Within a many-body Green's function theory a quantitative analysis of the interlayer exchange coupling J_{inter} and the shift $\Delta T_{C,Ni}(d_{Ni}, d_{Cu})$ is performed. Realistic values for J_{inter} are only obtained if the action of collective magnetic excitations is taken into account. By application of the GFT approach together with the expression by Bruno for the oscillatory IEC depending on the spacer layer thickness we are able to determine the full dependence of the IEC and the temperature shift as functions of the Ni and Cu film thicknesses, as summarized in the 3D-plot.

Note added in proof. Recently a work by J. Wu *et al.*⁴² came to our attention. This theoretical work is dealing with bilayers, i.e., two strongly coupled FM films. Within a mean field treatment the authors discuss two materials with different Curie temperatures. The calculated T_C would correspond to the T_C of our top Co film which is not addressed in the

present work for the following reason: Our Co T_C is larger than 300 K. Experiments at these high temperatures would lead to strong interdiffusion effects. However, we agree with the authors of Ref. 42 that the coupling of the two FM films can also influence the T_C of Co. But the major effect of giant spin fluctuations in 2D ferromagnets, as present in the trilayers investigated here, is evidenced at the lower $T_{C,Ni}^*$, i.e., the quasicritical temperature of Ni.

ACKNOWLEDGMENTS

We thank the BESSY crew for the excellent experimental conditions, in particular B. Zada. Ongoing discussions with W. Nolting and his coworkers are acknowledged. We thank O. Eriksson for the communication of Ref. 13 prior to publication. Support from BMBF (05 KS4 KEB/5) and DFG, Sfb 290 (TP A02 and TP A01) is gratefully acknowledged.

*Present address: SSRL, Stanford Linear Accelerator Center, 2575 Sand Hill Road, Menlo Park, California 94025.

†Corresponding author. Electronic address: babgroup@physik.fu-berlin.de; URL: <http://www.physik.fu-berlin.de/~ag-baberschke/index.html>

¹See, e.g., *Magnetism Beyond 2000*, edited by A. J. Freeman and S. D. Bader (North-Holland, Amsterdam, 1999).

²U. Bovensiepen, F. Wilhelm, P. Srivastava, P. Pouloupoulos, M. Farle, A. Ney, and K. Baberschke, *Phys. Rev. Lett.* **81**, 2368 (1998).

³P. Pouloupoulos and K. Baberschke, *Band-Ferromagnetism*, edited by K. Baberschke, M. Donath, W. Nolting, Lecture Notes in Physics, Vol. 580 (Springer, 2001), p. 283.

⁴see, e.g., *Ultrathin Magnetic Structures*, Vol. II, edited by B. Heinrich and J. A. C. Bland (Springer-Verlag, Berlin, 1994).

⁵J. Lindner and K. Baberschke, *J. Phys.: Condens. Matter* **15**, S465 (2003).

⁶G. Bayreuther, F. Bensch, and V. Kottler, *J. Appl. Phys.* **79**, 4509 (1996).

⁷P. Bruno and C. Chappert, *Phys. Rev. Lett.* **67**, 1602 (1991); **67**, 2592 (1991); P. Bruno, *Phys. Rev. B* **52**, 411 (1995).

⁸See, e.g., K. Baberschke, *Appl. Phys. A: Mater. Sci. Process.* **62**, 417 (1996); P. Pouloupoulos and K. Baberschke, *J. Phys.: Condens. Matter* **11**, 9495 (1999), and references therein.

⁹J. H. Wu, T. Herrmann, M. Potthoff, and W. Nolting, *J. Phys.: Condens. Matter* **12**, 2847 (2000).

¹⁰P. J. Jensen, K. H. Bennemann, P. Pouloupoulos, M. Farle, F. Wilhelm, and K. Baberschke, *Phys. Rev. B* **60**, R14994 (1999).

¹¹D. Kerkmann, D. Pescia, and R. Allenspach, *Phys. Rev. Lett.* **68**, 686 (1992).

¹²C. H. Back, Ch. Würsch, A. Vaterlaus, U. Ramsperger, U. Maier, and D. Pescia, *Nature (London)* **378**, 597 (1995).

¹³L. Bergqvist and O. Eriksson (unpublished).

¹⁴J. Lindner, P. Pouloupoulos, F. Wilhelm, M. Farle, and K. Baberschke, *Phys. Rev. B* **62**, 10431 (2000).

¹⁵J. Shen, J. Giergiel, and J. Kirschner, *Phys. Rev. B* **52**, 8454 (1995).

¹⁶A. Ney, A. Scherz, P. Pouloupoulos, K. Lenz, H. Wende, K. Baberschke, F. Wilhelm, and N. B. Brookes, *Phys. Rev. B* **65**, 024411 (2002).

¹⁷A. Ney, P. Pouloupoulos, and K. Baberschke, *Europhys. Lett.* **54**, 820 (2001).

¹⁸C. Won, Y. Z. Wu, A. Scholl, A. Doran, N. Kurahashi, H. W. Zhao, and Z. Q. Qiu, *Phys. Rev. Lett.* **91**, 147202 (2003); C. Won, Y. Z. Wu, N. Kurahashi, H. W. Zhao, Z. Q. Qiu, A. Scholl, and A. Doran, *ibid.* **94**, 039704 (2005).

¹⁹R. W. Wang and D. L. Mills, *Phys. Rev. B* **46**, 11681 (1992).

²⁰A. Scherz, F. Wilhelm, U. Bovensiepen, P. Pouloupoulos, H. Wende, and K. Baberschke, *J. Magn. Magn. Mater.* **236**, 1 (2001).

²¹A. Scherz, F. Wilhelm, P. Pouloupoulos, H. Wende, and K. Baberschke, *J. Synchrotron Radiat.* **8**, 472 (2001).

²²P. J. Jensen, C. Sorg, A. Scherz, M. Bernien, K. Baberschke, and H. Wende, *Phys. Rev. Lett.* **94**, 039703 (2005).

²³C. Sorg, A. Scherz, H. Wende, T. Gleitsmann, Z. Li, S. Rüttinger, Ch. Litwinski, and K. Baberschke, *Phys. Scr., T* **115**, 638 (2005).

²⁴F. Wilhelm, U. Bovensiepen, A. Scherz, P. Poloupoulos, A. Ney, H. Wende, G. Ceballos, and K. Baberschke, *J. Magn. Magn. Mater.* **222**, 163 (2000).

²⁵C. Rüdts, A. Scherz, and K. Baberschke, *J. Magn. Magn. Mater.* **285**, 95 (2004).

²⁶R. Ramchal, A. K. Schmid, M. Farle, and H. Poppa, *Phys. Rev. B* **68**, 054418 (2003).

²⁷P. J. Jensen, *Ann. Phys.* **6**, 317 (1997).

²⁸S. Schwieger, J. Kienert, and W. Nolting, *Phys. Rev. B* **71**, 024428 (2005).

²⁹S. V. Tyablikov, *Methods in the Quantum Theory of Magnetism* (Plenum, New York, 1967); P. Fröbrich, P. J. Jensen, and P. J. Kuntz, *Eur. Phys. J. B* **13**, 477 (2000).

³⁰A. M. N. Niklasson, B. Johansson, and H. L. Skriver, *Phys. Rev. B* **59**, 6373 (1999).

³¹H. B. Callen, *Phys. Rev.* **130**, 890 (1963).

³²S. V. Tyablikov, *Ukr. Mat. Zh.* **11**, 287 (1959).

³³T. Holstein and H. Primakoff, *Phys. Rev.* **58**, 1098 (1940).

³⁴A. Ney, F. Wilhelm, M. Farle, P. Pouloupoulos, P. Srivastava, and K. Baberschke, *Phys. Rev. B* **59**, R3938 (1999).

³⁵R. B. Griffiths, in *Phase Transition and Critical Phenomena*, Vol. I, edited by Domb and Green (Academic Press, 1972, London), p. 75.

³⁶M. Donath, D. Scholl, H. C. Siegmann, and E. Kay, *Phys. Rev. B* **43**, 3164 (1991).

³⁷In P. Bruno, *Eur. Phys. J. B* **11**, 83 (1999) an extension to the asymptotic expansion [Eq. (4)] for the ultrathin limit of the spacer thickness is given. However, we have demonstrated in earlier experimental works⁵ that at least the wave numbers and the phase shifts are valid in the range of $d_{Cu}=2-9$ ML. Furthermore, we see that the comparison of our model calculation shown in Fig. 8 is in fair agreement with the experimental data points. Therefore, we do not apply the extended model in the present study.

³⁸W. Weber, R. Allenspach, and A. Bischof, *Europhys. Lett.* **31**, 491 (1995).

³⁹R. Hammerling, J. Zabloudil, P. Weinberger, J. Lindner, E. Ko-

- subek, R. Nünthel, and K. Baberschke, Phys. Rev. B **68**, 092406 (2003).
- ⁴⁰M. Pajda, J. Kudrnovský, I. Turek, V. Drchal, and P. Bruno, Phys. Rev. Lett. **85**, 5424 (2000).
- ⁴¹P. Henelius, P. Fröbrich, P. J. Kuntz, C. Timm, and P. J. Jensen, Phys. Rev. B **66**, 094407 (2002).
- ⁴²J. Wu, S. Dong, and Xiaofeng Jin, Phys. Rev. B **70**, 212406 (2004).